



# A novel study of the effect of temperature on the crystal structure of lithium aluminosilicate materials

Rut Benavente<sup>a,\*</sup>, María Dolores Salvador<sup>a</sup>, Adolfo Fernandez<sup>b</sup>, Amparo Borrell<sup>a</sup>

<sup>a</sup> Instituto de Tecnología de Materiales (ITM), Universitat Politècnica de València, Camino de Vera, S/n, 46022, Valencia, Spain

<sup>b</sup> Nanomaterials and Nanotechnology Research Center (CINN-CSIC), Universidad de Oviedo (UO), Principado de Asturias (PA), Avda. de La Vega 4-6, 33940, El Entrego, Spain

## ARTICLE INFO

### Keywords:

β-eucryptite  
XRD  
Crystallinity  
Dilatometry  
Microwave sintering

## ABSTRACT

Dense Li<sub>2</sub>O–Al<sub>2</sub>O<sub>3</sub>–SiO<sub>2</sub> (LAS) material was obtained in solid state by two sintering methods: conventional and microwave. The cyclical variation in temperature that these materials are subjected to during their useful life could cause changes in their crystalline structure and therefore changing their macroscopic properties. The role played by temperature in the diffraction patterns evolution was investigated through X-Ray thermodiffraction measurements. Evolution of lattice parameters and crystal structure was determined and correlated with changes in the coefficient of thermal expansion. This work provides a comprehensive view of the thermal history of LAS materials according to the sintering technique used.

## 1. Introduction

The Li<sub>2</sub>O–Al<sub>2</sub>O<sub>3</sub>–SiO<sub>2</sub> (LAS) system has attracted much attention over recent decades due to its hexagonal crystal structure [1], resulting in a low or negative coefficient of thermal expansion (CTE) [2–5]. Therefore, the usefulness of these thermal properties in the production of materials with excellent mechanical properties, good thermal shock resistance, high thermal stability, and high chemical durability, makes them suitable for potential engineering applications where high dimensional stability is required during several heating cycles. These properties are influenced by the nature, morphology and volume fraction of the crystalline phases formed [6,7].

The thermal expansion behaviour of dense LAS materials over a wide temperature range, including cryogenic conditions has been well reported. Some studies have focused on the dimensional stability behaviour of these materials over time, with no loads or variable environmental conditions, but there are no previous literature results on the evolution of crystallographic parameters with temperature and its relation to the coefficient of thermal expansion during several heating cycles [8–10]. Hysteretic temperature effects can have a significant influence on the thermal history of the material crystalline structure.

García-Moreno et al. [11–14], reported very low or null thermal expansion materials from pure β-eucryptite phase with different compositions (Li<sub>2</sub>O:Al<sub>2</sub>O<sub>3</sub>:SiO<sub>2</sub> as 1:1:2; and 1:1:3.11) in dense ceramic

bodies in the solid state by sintering in conventional or spark plasma sintering. Benavente et al. [15], compared the influence of the sintering methodology (conventional and microwave sintering) on the thermal and mechanical properties of lithium aluminosilicate materials (β-eucryptite phase). These studies only focused on the heating modes and the most important characteristics associated with the sintering process that improve the final properties of the materials [16–18].

In this work, we carry out a novel study of the evolution of crystallographic parameters on the crystal structure of β-Eucryptite phase in the lithium aluminosilicate system and its relation to the coefficient of thermal expansion during several heating cycles in the temperature range of 25 °C–400 °C. This material was produced by either conventional or microwave sintering technology and characterised by thermodiffraction analysis. The crystal structure of Li<sub>2</sub>O–Al<sub>2</sub>O<sub>3</sub>–SiO<sub>2</sub> was refined by the Rietveld method. Furthermore, we focused on the effect of temperature on the change in crystal structure, by evaluating the thermal history depending on the sintering technique.

## 2. Materials and methods

The synthesised LAS powder material was obtained by following the procedure described in a previous work [19]. The chemical composition of the powder in terms of Li<sub>2</sub>O–Al<sub>2</sub>O<sub>3</sub>–SiO<sub>2</sub> relation is 1:1.1:2.5 and it relates to β-eucryptite crystalline phase.

\* Corresponding author.

E-mail address: [rutbmr@upvnet.upv.es](mailto:rutbmr@upvnet.upv.es) (R. Benavente).

<https://doi.org/10.1016/j.oceram.2021.100169>

Received 9 December 2020; Received in revised form 3 March 2021; Accepted 10 August 2021

Available online 13 August 2021

2666-5395/© 2021 The Authors. Published by Elsevier Ltd on behalf of European Ceramic Society. This is an open access article under the CC BY-NC-ND license

(<http://creativecommons.org/licenses/by-nc-nd/4.0/>).

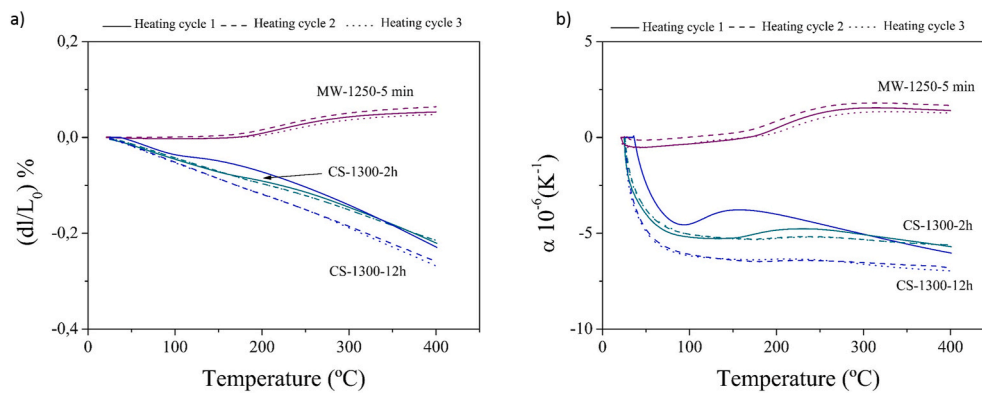


Fig. 1. a) Elongation vs. temperature and b) thermal expansion coefficient, of three thermal cycles, of MW-1250-5min, CS-1300-2h and CS-1300-12h and samples.

LAS powders were compacted by cold isostatic pressing (CIP) at 200 MPa of pressure (15 mm height, 10 mm diameter). The green density was approximately  $1.2 \text{ g cm}^{-3}$ , i.e. 49% of theoretical density ( $2.39 \text{ g cm}^{-3}$ ). Green samples were sintered using two different processing methods: conventional (CS) and microwave sintering (MW). Sintering conditions were fixed in accordance with the results of previous works [15,20], based on the coefficient of thermal expansion (CTE) behaviour, with the objective of obtaining samples with a near zero CTE. In the CS method, an electrical furnace (Thermolyne Type 46100, Thermo Fisher Scientific, USA) with  $10^\circ\text{C min}^{-1}$  of heating rate was used. Samples were heated at  $1300^\circ\text{C}$  in air with a dwell time of 2 and 12 h, and were then named CS-1300-2h and CS-1300-12h, respectively. Alternatively, a single mode cylindrical cavity operating in the TE<sub>111</sub> mode with a resonant frequency of 2.45 GHz was selected as the heating cell for microwave sintering [21]. The samples were sintered at  $1250^\circ\text{C}$  in air with a heating rate of  $100^\circ\text{C min}^{-1}$  with a short holding time of 5 min (MW-1250-5min) [15].

The bulk density of the sintered samples was measured by the Archimedes method in distilled water (ASTM C373-88).

The thermodiffractometric (TDX) studies were performed on a Bruker D8 Advance Vantec diffractometer equipped with a HTK 2000 variable temperature chamber (Germany). Patterns were obtained using Cu K $\alpha$  radiation. The measurements were performed in the  $15^\circ$ - $80^\circ$  range and the step size and time of reading were  $15^\circ$  and 0.03 s, respectively, at measurement intervals of  $50^\circ\text{C}$ . The temperature range ranged from room temperature to  $400^\circ\text{C}$ , with a heating rate of  $10^\circ\text{C min}^{-1}$ . Two cycles of heating and cooling were recorded for the starting powder and each sintered material.

Structural refinements were performed using the Rietveld method (external standard method) [22] in the programme cyclic FULLPROF option [23], in order to follow the thermal evolution of the cell parameters of each material and observe if any structural variation occurred. The obtained XRD patterns were indexed using the diffraction files of  $\beta$ -eucryptite (PDF: 870602).

The coefficient of thermal expansion was checked in a Netzsch DIL-402-C dilatometer (Germany) between  $25^\circ\text{C}$  and  $400^\circ\text{C}$ .

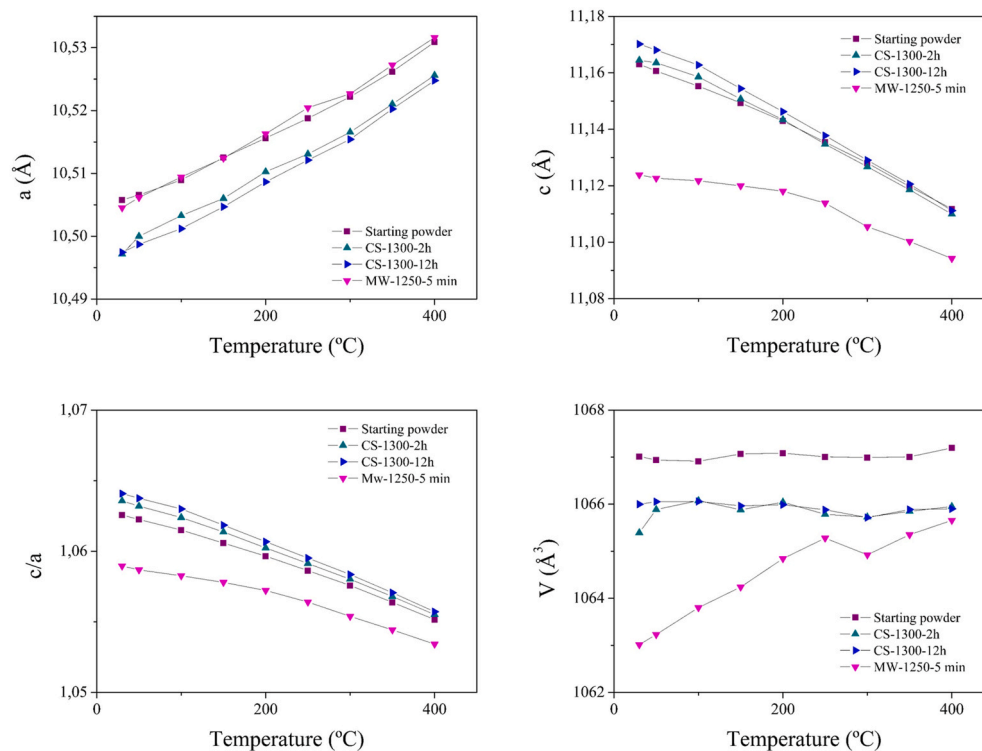


Fig. 2. Evolution of the crystallographic parameters  $a$ ,  $c$ ,  $c/a$  and  $V$  with temperature of the LAS starting powder and the sintered samples, CS-1300-2h, CS-1300-12h and MW-1250-5min.

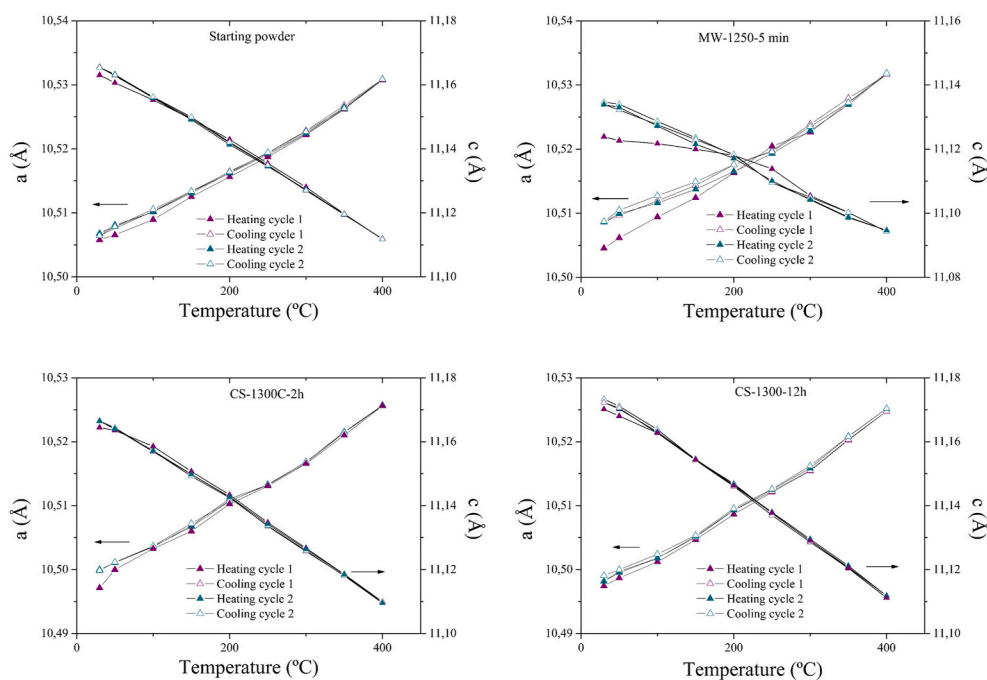


Fig. 3. Crystallographic parameters  $a$  and  $c$  evolution vs temperature during two heating cycles and two cooling cycles.

### 3. Results and discussion

The relative densities of sintered samples obtained by microwave sintering (MW-1250-5min) and conventional sintering at 1300 °C with 2h and 12h holding times (CS-1300-2h and CS-1300-12h) were around 99 %, 90 % and 96 %, respectively. The microwave-sintered samples show a relatively high density value, close to theoretical density, and enhanced by 9% compared with the CS-1300-2h samples. Despite the different density values of samples, we have chosen these materials based on previous study [15,20], where  $\beta$ -eucryptite material was obtained with glass-free.

The grain size of each sintered samples: MW-1250-5min, CS-1300-2h and CS-1300-12h is 2.1, 5.2 and 8.7  $\mu\text{m}$ , respectively [19,20]. This confirms that a 12 h dwelling time caused a grain thickening of  $\sim 40\%$  compared to the 2 h dwelling time sample, and  $\sim 75\%$  compared to SM-1250 °C-5min. This grain growth caused more microcracks at granular level, leading to more negative CTE values, as seen below [9, 10].

Dilatometric studies of the sintered samples were performed in the temperature range 25 to 400 °C. The dimensions of the tested samples were 12 x 10 x 3 mm. Three heating cycles were completed for each sample. Fig. 1a shows the dilatometry values of the samples, MW-1250-5min, CS-1300-2h and CS-1300-12h, vs. temperature. The microwave sintered sample showed more stable thermal behaviour with temperature in the three thermal cycles than conventional sintered samples. At macroscopic level, the thermal history of the material due to sintering process was noticeable in conventional sintering. That is, in both samples obtained by the conventional method, the second and third dilatometric cycles follow the same trend with temperature, while the first cycle differs from the other two. This difference between the first dilatometric cycle and the following ones is more noticeable as the sintering time increases.

In Fig. 1b, the CTE values of the samples MW-1250-5min, CS-1300-2h and CS-1300-12h are presented vs. temperature, calculated from the dilatometric curves. Previous works established the relationship between microcrack content and grain size, as well as with the sintering method used to obtain LAS materials [24]. A greater presence of microcracks and residual porosity promotes the decrease of the CTE

towards more negative values. The CS-1300-12h sample, with a longer sintering time, showed a more negative CTE than with a 2-h dwell time, which agrees with the presence of more microcracks. Moreover, thermal cycles promote this effect, especially in the case of conventional sintered samples.

Fig. 1b shows the different progress of the CTE values during the different thermal tests. These differences are noticeable in conventional sintering samples, in the first thermal cycle, with the CTE values being higher than in the following two cycles. In turn, this difference is more pronounced with increasing sintering dwelling times. In both cases, the CTE values of the first cycle are less negative than in subsequent cycles, and this would indicate a lower anisotropy in thermal expansion, that is, a greater structural disorder.

Another detail shown in Fig. 1b is the change in trend in the CTE values presented by all the samples tested. This change occurs at a higher temperature in the case of the sample sintered by microwave ( $\sim 250$  °C) compared to when obtained by conventional method ( $\sim 200$  °C). CS-1300-12h shows this change at lower temperature in the first cycle ( $\sim 150$  °C). The interpretation of this change in trend would be related to the variation in the crystallographic parameters  $a$  and  $c$ , and with the increase in temperature.

Fig. 2 show the evolution of the crystallographic parameters  $a$ ,  $c$ ,  $c/a$  and  $V$  with temperature obtained by Rietveld structural refinement of the LAS starting powder and the sintered samples, CS-1300-2h, CS-1300-12h and MW-1250-5min.

We can see the high anisotropy exhibited by  $\beta$ -eucryptite materials. Values of  $a$  crystallographic axis (axis equivalent to  $b$ ) increase with temperature, while  $c$ -axis values decrease for all materials tested [25, 26].

An important fact is the sintering process influence in these dimensional variations. The samples obtained by conventional technique show a similar behaviour despite the difference in processing time between them (2 and 12 h). However, the microwave sintered sample shows higher values of  $a$  and lower values of  $c$ . This results in a lower  $c/a$  ratio than in conventional sintered samples. Therefore, a lower value in  $c/a$  indicate an increase in the disorder of the structure, which cause a lower anisotropy in the expansion [6] and therefore, less negative CTE value as it was previously observed.

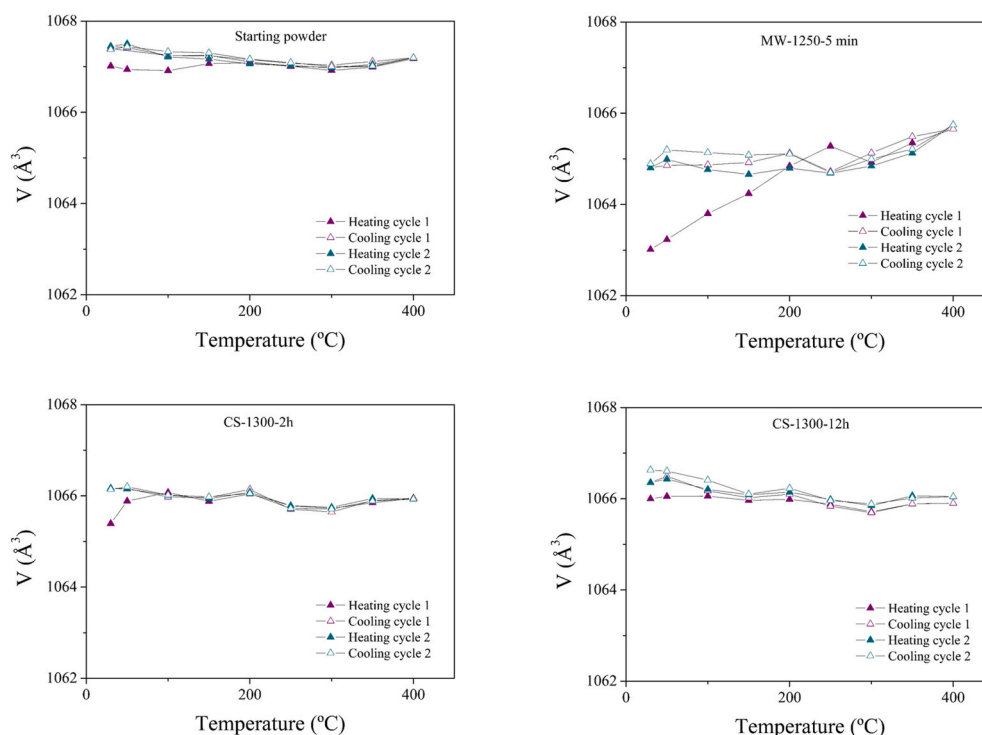


Fig. 4.  $V$  evolution vs temperature during two heating cycles and two cooling cycles.

The volume of the crystalline domain remains practically constant for the samples obtained by conventional sintering. However, the sample obtained by microwave sintering presents an increase in the crystalline volume with temperature, which is noticeable up to  $\sim 250$  °C. In Fig. 3, the evolution of the crystallographic parameters  $a$  and  $c$  as a function of temperature during two heating cycles and two cooling cycles is represented for each of the samples tested.

The sample sintered by microwave showed the highest thermal history. The values of the first heating were lower than those obtained in the first cooling cycle and in the following heating-cooling cycles down to  $\sim 250$  °C. Rapid cooling carried out in microwave sintering could cause the structure to freeze with more disorder than it would have at room temperature. By heating the sample again, with lower heating rates ( $10$  °C $\cdot$ min $^{-1}$ ), the crystalline structure is freed from the greater disorder it presents, thus freeing the structure from the thermal history of the material. In the following cooling and heating cycles, the crystallographic parameters evolve with the temperature following the same path.

In samples obtained by the conventional method, the thermal history of the material due to the sintering cycle was hardly noticeable, since the heating and cooling rates carried out in the sintering and in this study with temperature were the same ( $10$  °C min $^{-1}$ ).

Fig. 4 shows the crystalline domain volume evolution with temperature (by Rietveld analysis) during two heating cycles and two cooling cycles.

Crystallographic axes  $a$  and  $c$  show different behaviour in the first heating in the MW-1250-5min sample. As it could be expected, the volume increased considerably until it reached  $\sim 250$  °C, the temperature at which it started to stabilise. In the following cycles the volume remained relatively stable, except for the inflection point that takes place at  $\sim 250$  °C. As mentioned above, this inflection point may be due to the change in the ordered-disordered structure [6].

In the samples obtained by the conventional method, a slight difference was observed in the first heating cycle at low temperatures. The sintered sample with 2h dwell exhibited a more stable crystallographic behaviour with temperature than the 12h dwell sample, where a slight

increase in volume values was observed with increasing temperature cycles, despite the fact that the trend of the values was the same. In both cases, the volume values had an inflection point of  $\sim 200$  °C. This inflection point was not as pronounced as in the case of the sample obtained by microwave, occurring at a lower temperature.

#### 4. Conclusions

Summarising the above results, an important conclusion is that the order/disorder relationship in the structure of the  $\beta$ -eucryptite is dependent on the sintering method used. Consequently, the sample obtained by microwave needs a higher temperature to start to become disordered. In samples obtained by the conventional method, the larger the grain size, the lower the temperature needed to start observe changes.

This phenomenon appears to play a key role in results regarding the evolution of the crystallographic parameters with temperature and its relation to the coefficient of thermal expansion during several heating/cooling cycles. As an important result for future work, it has been demonstrated that the role of the electromagnetic field effect is very important for development materials for applications in which very controlled crystal structure and low thermal expansion behaviour are required at high temperatures.

#### Declaration of competing interest

The authors declare that they have no known competing financial interests or personal relationships that could have appeared to influence the work reported in this paper.

#### Acknowledgements

This research was funded by the project of the Spanish Ministry of Economy and Competitiveness (MINECO): RTI2018-099033-B-C32 and RYC-2016-20915.

## References

- [1] T. Ogiwara, Y. Noda, K. Shoji, O. Kimura, Low-temperature sintering of high-strength  $\beta$ -eucryptite ceramics with low thermal expansion using Li<sub>2</sub>O-GeO<sub>2</sub> as a sintering additive, *J. Am. Ceram. Soc.* 94 (2011) 1427–1433, <https://doi.org/10.1111/j.1551-2916.2010.04279.x>.
- [2] M. Chen, F. He, J. Shi, J. Xie, H. Yang, P. Wan, Low Li<sub>2</sub>O content study in Li<sub>2</sub>O-Al<sub>2</sub>O<sub>3</sub>-SiO<sub>2</sub> glass-ceramics, *J. Eur. Ceram. Soc.* 39 (2019) 4988–4995, <https://doi.org/10.1016/j.jeurceramsoc.2019.07.032>.
- [3] R.C. Cooper, G. Bruno, M.R. Wheeler, A. Pandey, T.R. Watkins, A. Shyam, Effect of microcracking on the uniaxial tensile response of  $\beta$ -eucryptite ceramics: experiments and constitutive model, *Acta Mater.* 135 (2017) 361–371, <https://doi.org/10.1016/j.actamat.2017.06.033>.
- [4] G. Li, R. Fu, S. Agathopoulos, X. Su, Q. He, Y. Ji, X. Liu, Ultra-low thermal expansion coefficient of PZB/ $\beta$ -eucryptite composite glass for MEMS packaging, *Ceram. Int.* 46 (2020) 8385–8390, <https://doi.org/10.1016/j.ceramint.2019.12.071>.
- [5] M. Suárez, A. Fernández, L.A. Díaz, I. Sobrados, J. Sanz, A. Borrell, F.J. Palomares, R. Torrecillas, J.S. Moya, Synthesis and sintering at low temperature of a new nanostructured beta-Eucryptite dense compact by spark plasma sintering, *Ceram. Int.* (2020), <https://doi.org/10.1016/j.ceramint.2020.04.152>, 0–1.
- [6] L.D. Wang, Z.W. Xue, Y. Cui, K.P. Wang, Y.J. Qiao, W.D. Fei, Thermal mismatch induced disorder of beta-eucryptite and its effect on thermal expansion of beta-eucryptite/Al composites, *Compos. Sci. Technol.* 72 (2012) 1613–1617, <https://doi.org/10.1016/j.compscitech.2012.06.013>.
- [7] R. Roy, D.K. Agrawal, H.A. McKinstry, Very low thermal expansion coefficient materials, *Annu. Rev. Mater. Sci.* 19 (1989) 59–81, <https://doi.org/10.1146/annurev.ms.19.080189.000423>.
- [8] Y. Bao, J. Yang, Y. Qiu, Y. Song, Space and time effects of stress on cracking of glass, *Mater. Sci. Eng.* 512 (2009) 45–52, <https://doi.org/10.1016/j.msea.2009.01.071>.
- [9] G. Bruno, V.O. Garlea, J. Muth, A.M. Efremov, T.R. Watkins, A. Shyam, Microstrain temperature evolution in  $\beta$ -eucryptite ceramics: measurement and model, *Acta Mater.* 60 (2012) 4982–4996, <https://doi.org/10.1016/j.actamat.2012.04.033>.
- [10] A. Shyam, J. Muth, E. Lara-Curzio, Elastic properties of  $\beta$ -eucryptite in the glassy and microcracked crystalline states, *Acta Mater.* 60 (2012) 5867–5876, <https://doi.org/10.1016/j.actamat.2012.07.028>.
- [11] O. García-Moreno, A. Fernández, R. Torrecillas, Conventional sintering of LAS-SiC nanocomposites with very low thermal expansion coefficient, *J. Eur. Ceram. Soc.* 30 (2010) 3219–3225, <https://doi.org/10.1016/j.jeurceramsoc.2010.07.003>.
- [12] O. García-Moreno, A. Fernández, R. Torrecillas, Solid state sintering of very low and negative thermal expansion ceramics by Spark Plasma Sintering, *Ceram. Int.* 37 (2011) 1079–1083, <https://doi.org/10.1016/j.ceramint.2010.11.035>.
- [13] O. García-Moreno, A. Fernández, R. Torrecillas, Sintering of mullite- $\beta$ -eucryptite ceramics with very low thermal expansion, *Int. J. Mater. Res.* 103 (2012) 416–421.
- [14] O. García-Moreno, A. Borrell, B. Bittmann, A. Fernández, R. Torrecillas, Alumina reinforced eucryptite ceramics: very low thermal expansion material with improved mechanical properties, *J. Eur. Ceram. Soc.* 31 (2011) 1641–1648, <https://doi.org/10.1016/j.jeurceramsoc.2011.03.033>.
- [15] R. Benavente, A. Borrell, M.D. Salvador, O. García-Moreno, F.L. Peñaranda-Foix, J. M. Catala-Civera, Fabrication of near-zero thermal expansion of fully dense  $\beta$ -eucryptite ceramics by microwave sintering, *Ceram. Int.* 40 (2014) 935–941, <https://doi.org/10.1016/j.ceramint.2013.06.089>.
- [16] C. Singhal, Q. Murtaza, Parvej, Microwave sintering of advanced composites materials: a review, *Mater. Today Proc.* 5 (2018) 24287–24298, <https://doi.org/10.1016/j.matpr.2018.10.224>.
- [17] M. Oghbaei, O. Mirzaee, Microwave versus conventional sintering: a review of fundamentals, advantages and applications, *J. Alloys Compd.* 494 (2010) 175–189, <https://doi.org/10.1016/j.jallcom.2010.01.068>.
- [18] K.I. Rybakov, E.A. Olevisky, E.V. Krikun, Microwave sintering: fundamentals and modeling, *J. Am. Ceram. Soc.* 96 (2013) 1003–1020, <https://doi.org/10.1111/jace.12278>.
- [19] O. García-Moreno, A. Fernández, S. Khainakov, R. Torrecillas, Negative thermal expansion of lithium aluminosilicate ceramics at cryogenic temperatures, *Scripta Mater.* 63 (2010) 170–173, <https://doi.org/10.1016/j.scriptamat.2010.03.047>.
- [20] R. Benavente, M.D. Salvador, O. García-Moreno, F.L. Peñaranda-Foix, J.M. Catala-Civera, A. Borrell, Microwave, spark plasma and conventional sintering to obtain controlled thermal expansion  $\beta$ -eucryptite materials, *Int. J. Appl. Ceram. Technol.* 12 (2015) E187–E193, <https://doi.org/10.1111/ijac.12285>.
- [21] F.L. Peñaranda-Foix, M.D. Janezic, J.M. Catala-Civera, A.J. Canos, Full-wave analysis of dielectric-loaded cylindrical waveguides and cavities using a new four-port ring network, *IEEE Trans. Microw. Theor. Tech.* 60 (2012) 2730–2740, <https://doi.org/10.1109/TMTT.2012.2206048>.
- [22] H.M. Rietveld, A profile refinement method for nuclear and magnetic structures, *J. Appl. Crystallogr.* 2 (1969) 65–71, <https://doi.org/10.1107/S0021889869006558>.
- [23] J. Rodríguez-Carvajal, Recent advances in magnetic structure determination by neutron powder diffraction, *Phys. B Condens. Matter* 192 (1993) 55–69, [https://doi.org/10.1016/0921-4526\(93\)90108-1](https://doi.org/10.1016/0921-4526(93)90108-1).
- [24] R. Benavente, M.D. Salvador, A. Martínez-Amesti, A. Fernández, A. Borrell, Effect of sintering technology in  $\beta$ -eucryptite ceramics: influence on fatigue life and effect of microcracks, *Mater. Sci. Eng.* 651 (2016) 668–674, <https://doi.org/10.1016/j.msea.2015.11.013>.
- [25] W.I. Abdel-Fattah, F.M. Ali, R. Abdellah, Lithia porcelains as promising breeder candidates — II. Structural changes induced by fast neutron irradiation, *Ceram. Int.* 23 (1997) 471–481, [https://doi.org/10.1016/S0272-8842\(96\)00055-7](https://doi.org/10.1016/S0272-8842(96)00055-7).
- [26] W.W. Pillars, The crystal structure of Beta eucryptite as a function of temperature, *Am. Mineral.* 58 (1973) 681–690.